The influence of weak texture on the critical currents in polycrystalline MgB_2

Eisterer M[1,*] and Weber H W[1]

[1] *Atominstitut, Vienna University of Technology, Stadionallee 2, 1020 Vienna*

Abstract

The current transport in polycrystalline MgB_2 is strongly influenced by the intrinsic anisotropy of this superconductor. Untextured bulks and wires are macroscopically isotropic, but the grains retain their anisotropic properties and the field dependence of the critical currents is much stronger than in isotropic superconductors. Weakly or partially textured tapes are macroscopically anisotropic, but the anisotropy of the zero resistivity (or irreversibility) field is smaller than the intrinsic upper critical field anisotropy, γ. The J_c-anisotropy is field and temperature dependent and can be much larger than γ. The most suitable parameter for the quantification of the macroscopic anisotropy is, therefore, the anisotropy of the zero resistivity field. It is difficult to distinguish between a higher degree of texture at a lower intrinsic anisotropy and a weaker texture at higher anisotropy and hardly possible based on the field dependence of the critical current anisotropy alone. The knowledge of the upper critical field is crucial and angular resolved measurements of either the critical currents or, better, the resistive in-field transitions are favorable for this purpose.

I. INTRODUCTION

A considerable anisotropy of the critical current is found in *ex-situ*[1–6] and *in-situ*[7,8] MgB_2 tapes. It is favored by a large aspect ratio of the tape, and is a consequence of the upper critical field anisotropy, γ, in magnesium diboride[9–13], if partial or weak texture is induced by the preparation technique. If the grain orientation is totally random (no texture), the conductor is macroscopically isotropic, since no preferred orientation exists. However, also in that case the intrinsic anisotropy of MgB_2 has severe consequences on the properties of polycrystalline materials. The critical current density, J_c, becomes zero well below the upper critical field, B_{c2}, which in turn leads to a much stronger field dependence of the critical current than in isotropic materials[14]. The Kramer plot is no longer linear near the irreversibility field and the peak of the volume pinning force shifts to significantly lower fields[15]. Large critical current densities of the order of $5 \times 10^8\,\mathrm{Am}^{-2}$ can be expected only up to[16] $B_{c2}^c = B_{c2}^{ab}/\gamma$, since only highly percolative currents flow on a macroscopic length scale at higher fields. B_{c2}^{ab} and B_{c2}^c denote the upper critical field, when the field is applied parallel and perpendicular to the boron planes, respectively. B_{c2}^{ab} is around 14 T at 0 K in clean MgB_2 and determines the upper critical field in untextured polycrystalline samples[16], if defined by a typical onset criterion (e.g. our definition in Sec. III). B_{c2}^c is not easily accessible in polycrystalline MgB_2 and only about 3 T at 0 K in the clean limit[9–12], which strongly restricts the field range for applications. Fortunately, B_{c2}^{ab} (and the upper critical field in polycrystalline samples) can be enhanced by impurity scattering[17–19], which also reduces γ[9,20]. Both changes enhance B_{c2}^c at low temperatures, which is good for applications. Impurity scattering is less effective in improving the properties at high temperatures, since it decreases the transition temperature[21] and this change offsets the other beneficial effects. Texturing the material might, therefore, be an interesting alternative for optimizing the material for application at higher temperatures and fields. It increases the in-field critical currents for one orientation at the expense of decreasing them in the other main orientation[22]. Texture is therefore only beneficial, if the tape is operated in or near the favorable orientation, which generally complicates the design of devices, but is certainly feasible in superconducting magnets.

Only weak texture was achieved in MgB_2 tapes so far, with the c-axis oriented preferentially perpendicular to the tape. The average misalignment angle of the *c*-axis from the tape normal was found to be rather high[5,23] (above 20°) compared to highly textured materials

(a few degrees only).

Weak texture is a unique property of some MgB_2 tapes, since the strongly anisotropic cuprate superconductors have to be highly textured for high intergranular currents[24,25] leading to a pronounced J_c-anisotropy. NbTi and Nb_3Sn on the other hand are isotropic superconductors, thus (weak) texture is not expected to influence the properties of wires or tapes. In this report the influence of weak texture on the macroscopic current transport in MgB_2 will be discussed and the resulting behavior compared to the limiting cases of zero or perfect texture.

II. THE MODEL

A general model for nonlinear transport in heterogeneous media was presented in Ref. 14. The critical current was obtained by integrating the percolation cross section, $\sigma_\mathrm{p} \propto (p(J) - p_\mathrm{c})^t$, over all possible local currents J. $p(J)$ was defined as the fraction of grains with a $J_\mathrm{c}^\mathrm{local}$ above J. The percolation threshold, p_c, depicts the minimum fraction of superconducting grains for a continuous path through the superconductor. The percolation cross section reduces to zero at p_c, which is expected to be around 0.25 in typical polycrystalline MgB_2 materials[14,26–28]. This value will be used in the following. The transport exponent, t, is expected to be 1.76[29], which will be assumed in the following, although higher values were also observed experimentally[26,30]. Furthermore, a model for the field dependence of the local critical currents is needed for calculating $p(J)$. Since grain boundary pinning is dominant in the majority of MgB_2 conductors[9,14,31], $J_\mathrm{c}^\mathrm{local} \propto (1-b)^2/\sqrt{B}$ was assumed[32], but contributions of point pins were also reported[33,34]. b denotes the magnetic field normalized by the (angular dependent) upper critical field of the grain. Finally, the anisotropic scaling approach[35] was used to model the angular dependence of the local critical currents. Note that we already had to make four approximations/assumptions (p_c, t, pinning model, anisotropic scaling), which influence the field dependence of J_c independently of the degree of texture.

Texture is a modification of the distribution function of the grains' orientation. For uniaxial texture and the present geometry (preferred c-axis orientation perpendicular to the tape), the density of grains with a certain orientation only depends on the angle α between the tape normal and the c-axis of the grains. The corresponding distribution function is a

priori unknown. A Gaussian-like exponential function

$$f_{\mathrm{a}}(\alpha) \propto \exp(-\frac{\alpha^2}{2\alpha_{\mathrm{t}}^2}) \tag{1}$$

was chosen, which was confirmed by high energy synchrotron x-ray diffraction measurements[23]. Since α is restricted to $[0, 90°]$, the density distribution function has to be renormalized numerically[22] and is formally not a true Gaussian distribution. This implies that α_{t} is no longer the standard deviation of the distribution or an average misalignment angle, which are restricted to angles below 90°, but only a parameter which characterizes the decrease of the density distribution function between 0 and 90° and, therefore, the degree of texture. α_{t} converges to zero in the limit of perfect texture and diverges in untextured materials (f_{a} becomes constant between 0 and 90° for $\alpha_{\mathrm{t}} \to \infty$, uniform distribution).

Only a few quantitative data about texture in MgB_2 tapes exist in the literature, varying between 20° and 30°[5,23], but the model is not restricted to this angular range. For $\alpha_{\mathrm{t}} \to 0$ and ∞, the results of the model merge the predictions of the anisotropic scaling approach[35] and the percolation model for untextured MgB_2[14], respectively.

For the calculation of the angular dependence of J_{c}, B_{c2} and $B_{\rho=0}$, the density distribution function with respect to the direction of the applied magnetic field is needed, which was derived from the distribution function Equ. 1 in Ref. 22. All following calculations are based on this density distribution function.

III. RESULTS AND DISCUSSION

At first we focus on the anisotropy of the zero resistivity (irreversibility) field $B_{\rho=0}$. This quantity is less model dependent than J_{c}. It is independent of the pinning mechanism, the transport exponent and anisotropic scaling. Only the angular dependence of the upper critical field has to be known. Good agreement with the theoretical prediction of the anisotropic Ginzburg Landau theory[36],

$$B_{\mathrm{c2}}(\theta) = B_{\mathrm{c2}}^{ab}/\sqrt{\gamma^2\cos^2(\theta) + \sin^2(\theta)}, \tag{2}$$

was demonstrated[10,13,37,38]. It was shown in Ref. 16, that $B_{\rho=0}$ in untextured materials is given by

$$B_{\rho=0} = \frac{B_{\mathrm{c2}}^{ab}}{\sqrt{(\gamma^2-1)p_{\mathrm{c}}^2+1}}. \tag{3}$$

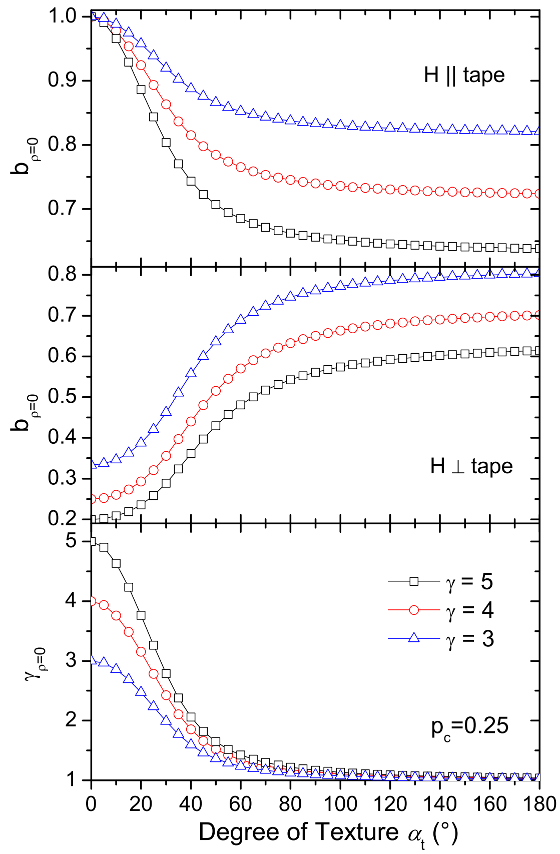

FIG. 1: The zero resistivity field in parallel orientation (top) increases with the degree of texture (decreasing α_t), but decreases in perpendicular orientation (middle). $B_{\rho=0}$ was normalized by B_{c2}^{ab} ($b_{\rho=0} := B_{\rho=0}/B_{\mathrm{c2}}^{ab}$). The anisotropy of $B_{\rho=0}$ varies between the intrinsic value at $\alpha_\mathrm{t} = 0$ and 1 in the untextured material (bottom). It changes strongest between 10° and 70°.

While B_{c2}^{ab} can be easily assessed experimentally, p_c[26] and γ[11] are difficult to determine. By fixing p_c to a realistic value, γ can be estimated from the difference between[39] $B_{\rho=0}$ and B_{c2}^{ab}, or, alternatively, by estimating γ from T_c, p_c can be obtained[9,26]. However, any uncertainty in one quantity induces a similar error in the other one; furthermore Equ. 3 was derived for a perfectly homogeneous material and neglecting the influence of thermal fluctuations. Both effects increase the difference between $B_{\rho=0}$ and B_{c2}. Thermal fluctuations, which result in a difference between the *intrinsic* B_{c2} and B_{irr} in each grain, generally increase with B_{c2} (the importance of fluctuations is quantified by the Ginzburg number[40] $Gi \propto B_{\mathrm{c2}}^3$) and T. A successful description of the resistive transition by Equ. 3 thus requires a homogeneous material (narrow superconducting zero field transition), a moderate upper critical field, and temperatures well below T_c.

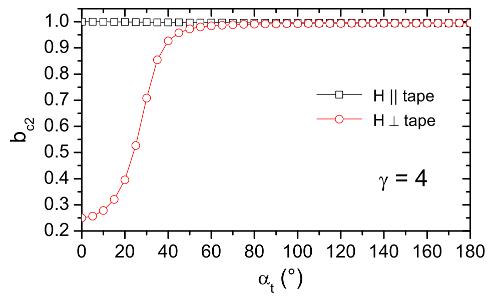

FIG. 2: The upper critical field is less sensitive to texture than $B_{\rho=0}$ (cf. Fig. 1). B_{c2} was normalized by B_{c2}^{ab} ($b_{\mathrm{c2}} := B_{\mathrm{c2}}/B_{\mathrm{c2}}^{ab}$) and refers to the onset of the superconducting transition.

Texture enhances $B_{\rho=0}$ (compared to the prediction of Equ. 3 for untextured $\mathrm{MgB_2}$), when the field is oriented parallel to the tape ($B_{\rho=0}^{\parallel}$, top panel in Fig. 1), but reduces $B_{\rho=0}$ in perpendicular orientation ($B_{\rho=0}^{\perp}$, middle panel) leading to an anisotropy of $B_{\rho=0}$, $\gamma_{\rho=0} := B_{\rho=0}^{\parallel}/B_{\rho=0}^{\perp}$ (bottom panel). The *intrinsic* anisotropy is obtained at $\alpha_{\mathrm{t}} = 0°$ (perfect texture), the anisotropy is very small at $\alpha_{\mathrm{t}} = 180°$ (1.02, 1.03, and 1.04 for $\gamma = 3$, 4, and 5, respectively).

The upper critical field is less sensitive to texture than $B_{\rho=0}$, as demonstrated for $\gamma = 4$ in Fig. 2. The data roughly correspond to a 90% resistive criterion, since a fraction of 2.5% superconducting grains was assumed for the calculations. If, say, 25% superconducting grains were needed for zero resistivity ($p_{\mathrm{c}} = 0.25$), around 2.5% should be enough to lower the resistivity by 10%. This definition (2.5% superconducting grains) will be used for the (angular dependent) upper critical field, B_{c2}, in the following. (Henceforth $B_{\mathrm{c2}}(\theta_{\mathrm{t}})$ always denotes this macroscopic upper critical and not the intrinsic $B_{\mathrm{c2}}(\theta)$ (Equ. 2) within the grains.) The upper critical field is nearly independent of texture, if the field is applied parallel to the tape. This is why the onset of the transition always corresponds to B_{c2}^{ab} in untextured materials. A significant anisotropy of the upper critical field is observed only for α_{t} below about 45°. The anisotropy of the upper critical field is only 1.4, while $\gamma_{\rho=0}$ is 2.4 at $\alpha_{\mathrm{t}} = 30°$.

The upper critical field and its anisotropy are much more sensitive to the chosen criterion than $B_{\rho=0}$ and $\gamma_{\rho=0}$. Therefore, and because of the field and temperature dependence of the J_{c}-anisotropy (see below), $\gamma_{\rho=0}$ is the most useful parameter for the quantification of the

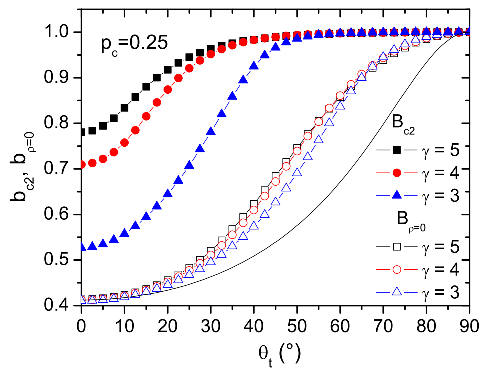

FIG. 3: Angular dependence of the upper critical field and the zero resistivity field. θ_t denotes the angle between the tape normal and the applied magnetic field. B_c2 and $B_{\rho=0}$ were normalized by their values at 90°. The $B_{\rho=0}$-anisotropy was fixed to 2.4 which corresponds to $\alpha_\mathrm{t} = 34.5$, 30, and 20.8° for $\gamma = 5$, 4, and 3, respectively. Neither B_c2 nor $B_{\rho=0}$ obey the angular dependence predicted by anisotropic Ginzburg Landau theory (solid line).

macroscopic anisotropy.

The same $\gamma_{\rho=0}$ (2.4) can be obtained with $\gamma = 5$ and $\alpha_\mathrm{t} = 34.5°$ or with $\gamma = 3$ and $\alpha_\mathrm{t} = 20.8°$. The corresponding angular dependencies of $B_{\rho=0}$ are presented in Fig. 3 (open symbols). They are similar to each other and cannot be described by the angular dependence predicted by anisotropic Ginzburg Landau theory (Equ. 2, line graph) by assuming $\gamma_{\rho=0}$ instead of γ. The deviation from this theory is even more pronounced for the onset of the transition (B_c2, solid symbols) and the anisotropy of the upper critical field is quite different at the same $B_{\rho=0}$-anisotropy. It seems therefore possible to estimate the three unknown parameters (γ, α_t, and p_c) from the angular dependence of $B_{\rho=0}$ and B_c2 and from the ratio of these quantities (not visible in Fig. 3, because the data were normalized by the values in parallel orientation).

The increase of $B_{\rho=0}$ in parallel orientation as well as the decrease in perpendicular orientation (compared to untextured materials) lead to a weaker and stronger field dependence of the critical currents, respectively (Fig. 4). While J_c converges to the limiting behaviour of perfect texture ($\alpha_\mathrm{t} = 0°$) rather quickly in the perpendicular orientation, it remains significantly below its limit in the parallel orientation, even for a high degree of texture ($\alpha_\mathrm{t} = 5°$). However, for a typical texture of $\alpha_\mathrm{t} = 20$–$30°$[5,23], a quite significant enhancement beyond

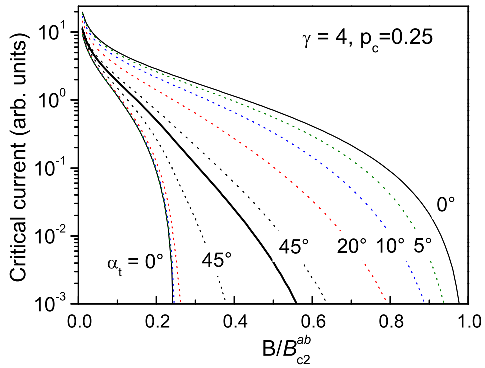

FIG. 4: Influence of texture on the critical currents. The thick solid line refers to untextured material ($\alpha_\mathrm{t} \to \infty$), dotted lines above and below to the parallel and perpendicular field orientation, respectively.

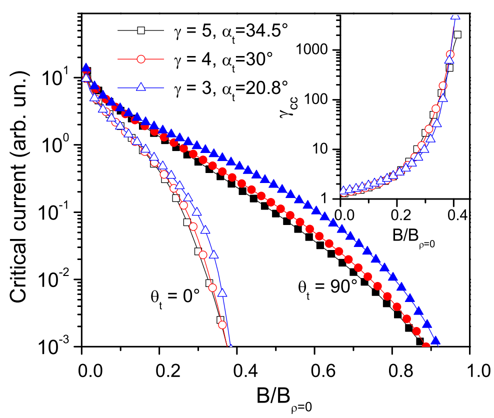

FIG. 5: Critical currents in materials with the same anisotropy of $B_{\rho=0}$ ($\gamma_{\rho=0} = 2.4$), but different degree of texture and intrinsic anisotropy γ. The magnetic field is normalized by the zero resistivity field in parallel field configuration. The inset presents the anisotropy of the critical currents γ_cc.

untextured materials can be expected at $B = B_{\mathrm{c2}}^{ab}/2$ in the parallel orientation.

Next we consider the influence of different combinations of γ and α_t, which lead to the same $\gamma_{\rho=0} = 2.4$, on the field dependence of J_c (Fig. 5). Although the results are slightly changed, the differences are not sufficient to derive these two parameters from $J_\mathrm{c}(B)$ alone, since they are also influenced by the usually unknown percolation threshold, the transport

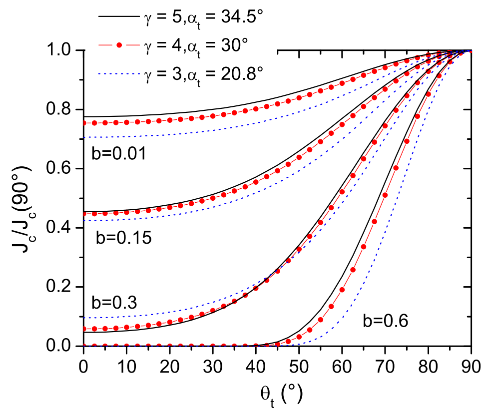

FIG. 6: The angular dependence of J_c is altered by different combinations of γ and α_t, which lead to the same anisotropy of the zero resistivity field, $B_{\rho=0}$ ($\gamma_{\rho=0} = 2.4$). The reduced fields, b, were normalized to $B_{\rho=0}$ in parallel orientation.

exponent, the pinning model and the angular dependence of $J_\mathrm{c}^\mathrm{local}$. Moreover $J_\mathrm{c}(B)$ is usually not available over four orders of magnitude. Note on the other hand that $B_{\rho=0}^{\parallel}/B_\mathrm{c2}^{ab}$ is different (0.7, 0.8, and 0.91 for $\gamma/\alpha_\mathrm{t} = 5/34.5°, 4/30°$, and $3/20.8°$, respectively), which cannot be seen in Fig. 5 due to the normalization. The knowledge of the upper critical field is therefore vital for the distinction between γ and α_t. Unfortunately, the metal sheath of tapes usually masks the onset of the transition[16] and must be removed for the determination of B_c2.

The anisotropy of the critical current is strongly field dependent (inset in Fig. 5) and diverges at $B_{\rho=0}^{\perp}$ ($B_{\rho=0}$ in orthogonal orientation). At fixed reduced field, $B/B_{\rho=0}$, it is not very sensitive to changes of the parameters, as long as the $B_{\rho=0}$-anisotropy is kept constant and is, therefore, also not appropriate for a (simultaneous) determination of γ and α_t. Since the field dependence of the critical current anisotropy scales with the upper critical field, the critical current anisotropy is also temperature dependent, because the reduced magnetic field increases with temperature at fixed magnetic field (B_c2 decreases).

The angular dependence of J_c is presented in Fig. 6. The same combinations of γ and α_t as for the field dependence of J_c were used. Data at the same reduced field, $b = B/B_{\rho=0}^{\parallel}$ are compared. The differences between $\gamma = 4$ and $\gamma = 5$ are small, but the curve for $\gamma = 3$ differs more significantly, which favors the analysis of texture from angular resolved measurements of J_c. However, the higher degree of modeling (pinning mechanism, percolation cross section,

anisotropic scaling) renders this procedure less reliable than measurements of the resistive transitions (without sheath) at various angles.

The data in Fig. 6 can be fitted to the behaviour predicted by the anisotropic scaling approach[35] for perfectly textured materials, with B_{c2} and γ as free parameters (not shown in Fig. 6). However, the obtained parameters do not have any physical meaning, because they change with field and strongly underestimate the real $B_{\rho=0}$ ($< B_{c2}$) and $\gamma_{\rho=0}$ ($< \gamma$).

IV. CONCLUSIONS

The influence of homogeneous weak texture on the macroscopic currents in MgB_2 was investigated on the basis of a percolation model for nonlinear transport in heterogeneous media. While any texture leads to an anisotropy of the zero resistivity field, the occurrence of a macroscopic upper critical field anisotropy (onset of the superconducting transition) indicates a significant degree of texture. Although the calculations were based on the anisotropic scaling approach for the intrinsic properties, the angular dependence of the macroscopic quantities (i.e., critical current, zero resistivity field, and upper critical field) do not obey the predictions of this general scaling in weakly textured materials, even if an effective instead of the intrinsic anisotropy is assumed.

It is hardly possible to derive the degree of texture and the intrinsic anisotropy from the field dependence of the critical current, in particular, if the upper critical field is unknown. Angular resolved measurements of the resistive transition turn out to be more appropriate for this purpose, but usually require the removal of the sheath.

The most suitable parameter for the quantification of the macroscopic anisotropy is the anisotropy of the zero resistivity field.

---

* Electronic address: eisterer@ati.ac.at

[1] Grasso G, Malagoli A, Marré D, Bellingeri E, Braccini V, Roncallo S, Scati N, and Siri A S 2002 *Physica* C **378-381** 899

[2] Kitaguchi H and Kumakura H 2005 *Supercond. Sci. Technol.* **18** S284

[3] Lezza P, Gladyshevskii R, Senatore C, Cusanelli G, Suo H L, and Flükiger R 2005 *IEEE Trans. Appl. Supercond.* **15** 3196

[4] Beilin V, Lapides I, Roth M, Dul´kin E, Mojaev E, Gerber A, and Riss O 2006 *J. Appl. Phys.* **100** 043903

[5] Lezza P, Gladyshevskii R, Abächerli V, and Flükiger R 2006 *Supercond. Sci. Technol.* **19** 286

[6] Serrano G, Serquis A, Civale L, Maiorov B, Malachevsky M T, and Ayala C 2008 *J. Phys.: Conf. Ser.* **97** 012129

[7] Kováč P, Melišek T, and Hušek I 2005 *Supercond. Sci. Technol.* **18** L45

[8] Kováč P, Hušek I, Dobročka E, Melišek T, Haessler W, and Herrmann M 2008 *Supercond. Sci. Technol.* **21** 015004

[9] Eisterer M 2007 *Supercond. Sci. Technol.* **20** R47

[10] Lyard L, Samuely P, Szabo P, Klein T, Marcenat C, Paulius L, Kim K H P, Jung C U, Lee H-S, Kang B, Choi S, Lee S-I, Marcus J, Blanchard S, Jansen A G M, Welp U, Karapetrov G, and Kwok W K 2002 *Phys. Rev.* B **66** 180502(R)

[11] Bud'ko S L and Canfield P C 2002 *Phys. Rev.* B **65** 212501

[12] Welp U, Rydh A, Karapetrov G, Kwok W K, Crabtree G W, Marcenat Ch, Paulius L, Klein T, Marcus J, Kim K H P, Jung C U, Lee H-S, Kang B, and Lee S-I 2003 *Phys. Rev.* B **67** 012505

[13] Angst M, Puzniak R, Wisniewski A, Jun J, Kazakov S M, Karpinski J, Roos J, and Keller H 2002 *Phys. Rev. Lett.* **88** 167004

[14] Eisterer M, Zehetmayer M, and Weber H W 2003 *Phys. Rev. Lett.* **90** 247002

[15] Eisterer M. 2008 *Phys. Rev.* B **77** 144524

[16] Eisterer M, Krutzler C, and Weber H W 2005 *J. Appl. Phys.* **98** 033906

[17] Gurevich A 2003 *Phys. Rev.* B **67** 184515

[18] Eisterer M, Müller R, Schöppl R, Weber H W, Soltanian S, and Dou S X 2007 *Supercond. Sci. Technol.* **20** 117

[19] Putti M et al. 2005 *Appl. Phys. Lett.* **86** 112503

[20] Krutzler C, Zehetmayer M, Eisterer M, Weber H W, Zhigadlo N D, and Karpinski J 2007 *Phys. Rev.* B **75** 224510

[21] Putti M, Brotto P, Monni M, Galleani E, Sanna A, and Massidda S 2007 *Eurohys. Lett.* **77** 57005

[22] Eisterer M, Häßler W, and Kováč P 2009 *Phys. Rev.* B **80** 174516

[23] Häßler W et al. to be published

[24] Durrell J H and Rutter N A 2009 *Supercond. Sci. Technol.* **22** 013001

[25] Feldmann D M, Holesinger T G, Feenstra R, and Larbalestier D C 2008 *J. Am. Ceram. Soc.* **91** 1869

[26] Eisterer M, Emhofer J, Sorta S, Zehetmayer M, and Weber H W 2009 *Supercond. Sci. Technol.* **22** 034016

[27] Yamamoto A, Shimoyama J-i, Kishio K, and Matsushita T 2007 *Supercond. Sci. Technol.* **20** 658

[28] Grinenko V, Krasnoperov E P, Stoliarov V A, Bush A A, and Mikhajlov B P 2006 *Solid State Comm.* **138** 461

[29] *Percolation Structure and Processes* Deutscher G, Fallen R, and Adler J 1983 Bristol: Adam Hilger

[30] Vionnet-Menot S, Grimaldi C, Maeder T, Strässler S, and Ryser P 2005 *Phys. Rev.* B **71** 064201

[31] Martínez E, Mikheenko P, Martínez-López M, Millán A, Bevan A, and Abell J S 2007 *Phys. Rev.* B **75** 134515

[32] Dew-Hughes D 1974 *Phil. Mag.* **30** 293

[33] Pallecchi I et al. 2005 *Phys. Rev.* B **71** 212507

[34] Chen J, Ferrando V, Orgiani P, Pogrebnyakov A V, Wilke R H T, Betts J B, Mielke C H, Redwing J M, Xi X X, and Li Qi 2006 *Phys. Rev.* B **74** 174511

[35] Blatter G, Geshkenbein V B, and Larkin A I 1992 *Phys. Rev. Lett.* **68** 875

[36] Tilley D R 1965 *Proc. Phys. Soc.* (London) **86** 289

[37] Rydh A, Welp U, Koshelev A E, Kwok W K, Crabtree G W, Brusetti R, Lyard L, Klein T, Marcenat C, Kang B, Kim K H, Kim K H P, Lee H S, and Lee S I 2004 *Phys. Rev.* B **70** 132503

[38] Prischepa S L, Della Rocca M L, Maritato L, Salvato M, Di Capua R, Maglione M G, and Vaglio R 2003 *Phys. Rev.* B **67** 024512

[39] Kim J H, Dou S X, Oh S, Jerčinović M, Babić E, Nakane T, and Kumakura H 2008 *J. Appl. Phys.* **104** 063911

[40] Brandt E H 1995 *Rep. Prog. Phys.* **58** 1465